

The two-qubit amplitude damping channel: characterization using quantum stabilizer codes

S. Omkar,^{1,*} R. Srikanth,^{2,†} Subhashish Banerjee,^{3,‡} and Anil Shaji^{1,§}

¹*School of Physics, IISER TVM, CET Campus, Thiruvananthapuram 695016, Kerala, India*

²*Poornaprajna Institute of Scientific Research, Sadashivnagar, Bengaluru- 560080, India*

³*Indian Institute of Technology Rajasthan, Jodhpur- 342011, India*

(Dated: November 12, 2015)

A protocol based on quantum error correction based characterization of quantum dynamics (QECCD) is developed for quantum process tomography on a two-qubit system interacting dissipatively with a vacuum bath. The method uses a 5-qubit quantum error correcting code that corrects arbitrary errors on the first two qubits, and also saturates the quantum Hamming bound. The dissipative interaction with a vacuum bath allows for both correlated and independent noise on the two-qubit system. We study the dependence of the degree of the correlation of the noise on evolution time and inter-qubit separation.

PACS numbers:

I. INTRODUCTION

Quantum error correction (QEC) is crucial for realizing quantum information protocols in the laboratory [1, 2]. Error correcting codes are designed specifically to both detect and correct for various types of errors that may occur during implementation of such protocols. Recently it was shown [3] that the error detection capabilities which are an integral part of the design of error correction codes can be leveraged to perform process tomography on a register of qubits. The noise process acting on the register is treated as the error and, in turn, error detection is done by initializing the register in suitable QEC code states. The statistics of the errors that are detected during QEC revealing the noise process is the idea behind the quantum error correction based characterization of dynamics (QECCD).

Characterizing the noise process is the first step in combating the environment induced loss of coherence and entanglement that almost always beset laboratory implementations of quantum information processing protocols [4]. It can actually determine the strategies to be adopted towards the fault tolerant quantum computation [5]. Such characterization of the dynamics of an open quantum system goes by the name of quantum process tomography [2]. In information processing scenarios, quantum process tomography also helps in benchmarking the fidelity of implementation of quantum gates [6] in addition to revealing the nature of the noise on the system.

A distinct advantage that QECCD has compared to other quantum process tomography techniques is that it can call upon the extensive body of literature available

on QEC for choosing optimal initial states for the register, useful measurements for syndrome detection etc. Additionally, once the noise process is identified, QEC techniques provide the means to cancel out the detrimental effect of the noise as well. The choice of the type of error correcting code to be employed for process tomography depends on the nature of the physical system that is being studied as well as the type of errors that are expected. For instance QEC codes like CSS codes [2] and five qubit codes [7] are designed to perform error correction when the noise on the register of qubits is uncorrelated. For correlated noise models, under some restricted conditions, codes like the ones in [8, 9] may be used. In this Paper we address the problem of characterizing noise acting on a pair of qubits that may or may not be correlated using QECCD.

We completely characterize the dissipative noise, due to interaction with a vacuum bath, on a two-qubit system [10, 11] using the QECCD. This noise model allows for both correlated and uncorrelated noise on the two-qubit system depending on the spatial separation between them. Using QECCD we reconstruct the quantum process matrix that describes the noise. The correlated nature of the noise makes the corresponding process matrix describing the noise non-factorizable. We also show that the non-classical correlations characterized by quantum discord [12, 13] will be generated between the two qubits due to time evolution under a correlated noise even if the qubits are initially in an uncorrelated product form.

The rest of this Paper is structured as follows. In the next section we briefly discuss open quantum dynamics, various methods of doing process tomography with emphasis on QECCD. In Sec. III, the dissipative noise on two qubits due to interaction with a vacuum bath is described. We quantify the degree of correlation of multi-qubit noise as a departure of the process matrix from product form, in Sec. IV. The characterization of the two-qubit noise is done next in Sec. V, where all the elements of the process matrix, characterizing the noise,

*Electronic address: omkar@iisertvm.ac.in

†Electronic address: srik@poornaprajna.org

‡Electronic address: subhashish@iitj.ac.in

§Electronic address: shaji@iisertvm.ac.in

are worked out. Sec. VI contains a brief discussion of our results.

II. OPEN QUANTUM DYNAMICS AND QECCD

The noise, \mathcal{E} acting on an open quantum system starting initially in a product state with its environment is described by a completely positive (CP), trace preserving dynamical map [14]. The dynamical map on a quantum state ρ of dimension d admits several representations. One such representation is in terms of a super-operator:

$$\rho' = \mathcal{E}(\rho) = \mathcal{A}\tilde{\rho}, \quad (1)$$

where $\tilde{\rho}$ is a $d^2 \times 1$ dimensional 'vectorized' version of ρ and \mathcal{A} is a super-operator with a $d^2 \times d^2$ matrix representation. Alternatively the map can be represented employing an operator sum representation [15],

$$\rho' = \mathcal{E}(\rho) = \sum_k K_j \rho K_j^\dagger,$$

where the Kraus operators, K_j satisfy $\sum_j K_j^\dagger K_j = \mathbb{1}_d$, for trace preserving map with $\mathbb{1}_d$ being the identity operator of dimension d . The operators K_j can be expanded in terms of a fixed set of trace-orthonormal operators F_l , which form a basis for the set of all operators on the state space of the open system as $K_j = \sum_l f_{jl} F_l$. The dynamical map can then be expressed in the fixed basis as

$$\rho' = \mathcal{E}(\rho) = \sum \chi_{l,m} F_l \rho F_m^\dagger, \quad (2)$$

with

$$\chi_{l,m} = \sum_j f_{jl} f_{jm}^*.$$

The dimensions of the process matrix $\chi_{l,m}$ is $d^2 \times d^2$. However, since \mathcal{E} is trace preserving, there are d^2 constraints on $\chi_{l,m}$ given by $\sum_{lm} \chi_{l,m} F_l^\dagger F_m = \mathbb{1}_d$, leading to $d^4 - d^2$ independent real elements for the process matrix. In this work the basis $\{F_l\}$ has multi-qubit Pauli operators (string of X , Y , Z and $\mathbb{1}_2$) as the elements and is known as the *error basis* being appropriate for employing the QEC formalism.

In quantum process tomography, the dynamical map is reconstructed from observations by either obtaining the elements of $\chi_{l,m}$ or by obtaining the Kraus operators or else, in some cases, by reconstructing the matrix representing the super-operator A . Other useful representations of the map like the operator sum-difference representation (OSDR) also exist [16]. In standard quantum process tomography [2, 17], a set of suitably prepared states $\{\rho_i\}$ are input to an unknown noisy dynamics \mathcal{E} to be characterized and the corresponding final states ρ_f are measured using state tomography. Repeating this

process for a sufficiently large number of linearly independent input states ρ_i the elements of $\chi_{l,m}$ can be obtained. Typically the number of measurements required to reconstruct the process scales as d^4 where d is the dimension of the quantum system of interest. Note that typically the system of interest is a register of n qubits whose Hilbert space dimension scales as 2^n and for such systems, the resources required to perform full process tomography scales exponentially with n as 2^{4n} .

There are several refinements on standard quantum process tomography with more favourable scalings of the resources (number of measurements) required to reconstruct a dynamical map. In ancilla assisted quantum process tomography, an ancillary system is added to the quantum system of interest and initialized in possibly entangled states with again possibly non-separable measurements on both system and ancilla following the action of the unknown dynamics on the system. Reconstruction of $\chi_{l,m}$ is then possible with d^2 measurements [18–20]. Direct characterization of quantum dynamics [21, 22] bypasses the many instances of state tomography needed in standard and ancilla assisted process tomography and the complete process matrix can be determined using d^2 different input states and only single measurements on each state. Other techniques includes characterization of the noise using an efficient method for transforming a quantum channel or process into a symmetric channel having only diagonal elements in the process matrix via twirling [23, 24]. A method similar to [23], but extended to estimate any given off-diagonal term, was introduced in [25] and it was further extended to perform process tomography with out using any ancilla in [26].

A. QECCD

In QECCD, the system of interest is a register of p qubits. A register of n qubits ($n > p$) is initialized into a QEC code state of the form

$$|\Psi_L\rangle \equiv \sum_{j=0}^{2^k-1} \beta_j |j_L\rangle, \quad (3)$$

where $\{|j_L\rangle\}$ denotes a logical basis for the code space of a $[[n, k]]$ QEC code which encodes k qubits into n . The first p qubits of the quantum register form the principal system \mathbf{P} of dimension $d = 2^p$ and the remaining $q = n - p$ qubits form an ancilla \mathbf{A} .

The size of the ancilla, q , is determined by the error correcting properties of the particular QEC code that is employed and it is chosen such that all the $4^p = d^2$ errors on \mathbf{P} can be detected and corrected. Hence the quantum register should satisfy the Hamming bound [27]

$$2^k 4^p \leq 2^{p+q}, \quad (4)$$

from which we have $q \geq p + k$. For the case where the bound in (4) is saturated and $k = 1$ we have $q = p + 1$. We

have made the assumption that there are no appreciable errors on ancillary qubits. However, the assumption can be relaxed using the ambiguous quantum error correcting codes [28] at the cost of having to do multiple initial state preparations of the n qubit register.

The underlying open quantum dynamics of \mathbf{P} determine the statistics of errors on the n qubit register. Note that we are, for simplicity, assuming that the noise alone is the dynamics of the register and deterministic evolution, if any, of the register is either trivial or alternatively, the discussion is set in an appropriate frame in which such evolution is trivial. While the choice of the QEC code determines the ‘errors’ that can be detected, we use the stabilizer formalism [2, 27, 29] for measuring the error statistics thereby revealing the elements of the process matrix χ . The stabilizers S_j are a set of $n-k$ mutually commuting binary n -qubit Pauli observables that stabilize the code space i.e.,

$$S_j|j_L\rangle = |j_L\rangle. \quad (5)$$

Any error given by the action of the operator F_j on the qubit register can be detected and hence corrected if for any pair F_j, F_k ($j \neq k$), there exists at least one S_l that anti-commutes with the product $F_j F_k$. This ensures that the set of measurement outcomes of the stabilizers S_l ’s, collectively forming the error syndrome, will be distinct for every pair F_j and F_k leading to unambiguous error detection. The stabilizer measurement collapses the noisy state into the pure state $|\Psi_L^x\rangle \equiv F_x|\Psi_L\rangle$, where F_x is the error that is detected and this state can be corrected by applying $F_x^\dagger = F_x$ to bring back the QEC code to its initial state.

1. Diagonal terms of χ .

The probability to obtain syndrome x corresponding to a error F_x on the quantum register is

$$\begin{aligned} \xi(x) &= \text{Tr}(\mathcal{E}(|\Psi_L\rangle\langle\Psi_L|)|\Psi_L^x\rangle\langle\Psi_L^x|) \\ &= \langle\Psi_L^x| \left[\sum_{l,m=0}^{d^2-1} \chi_{l,m} |\Psi_L^l\rangle\langle\Psi_L^m| \right] |\Psi_L^x\rangle \\ &= \sum_{l,m=0}^{d^2-1} \chi_{l,m} \delta_{x,l} \delta_{x,m} = \chi_{x,x}. \end{aligned} \quad (6)$$

From Eq. (6) it is clear that the diagonal element of the process matrix $\chi_{x,x}$ is nothing but the probability with which error F_x occurs. The error statistics and the probability for each detectable error characterized by syndrome x can be found by repeating the stabilizer measurements on the register after \mathbf{P} is subject to the noise. These measurements, done on the register a fixed number of times depending on the desired accuracy, yields all the d^2 diagonal terms of the process matrix corresponding

to unknown dynamics \mathcal{E} . Since all the S_j ’s are mutually commuting it is possible to obtain all the measurement outcomes simultaneously on a single state preparation. Every syndrome measurement must be followed by appropriate error correction steps if one is to bring the quantum register to its initial state.

2. Off-diagonal terms of χ .

To determine the $d^4 - 2d^2 + 1$ independent off-diagonal terms of a process matrix one has to pre-process the noisy quantum register with a suitable unitary operator $U(a, b)$ after the action of the noise, but before measuring the stabilizers. It is to be noted that pre-processing with any unitary rotates the set of correctable states to another set of correctable states without altering the error correction capability of the QEC code [3]. This means that the syndrome detection using stabilizer measurements and error correction can be performed as described earlier in Sec. II A 1.

Now consider the unitary operators,

$$\begin{aligned} U(a, b) &= \frac{F_a + F_b}{\sqrt{2}} \quad \text{if} \quad \{F_a, F_b\} = 0 \\ U(a, b) &= \frac{F_a + iF_b}{\sqrt{2}} \quad \text{if} \quad [F_a, F_b] = 0 \end{aligned} \quad (7)$$

such that $F_a F_x$ and $F_b F_x$ represent correctable errors on \mathbf{P} of the quantum register. Let $g_A F_A \equiv F_a F_x$, where F_A is a Pauli group operator and the *Pauli factor* $g_A \in \{\pm 1, \pm i\}$. Similarly, let $g_B F_B \equiv F_b F_x$.

The probability that the stabilizer measurements find error syndrome x on the quantum register preprocessed, prior to measurement, with the unitary operator $U(a, b) = (F_a + F_b)/\sqrt{2}$ is

$$\begin{aligned} \xi(a, b, x) &\equiv \text{Tr}(U(a, b)\mathcal{E}(|\Psi_L\rangle\langle\Psi_L|)(U(a, b))^\dagger|\Psi_L^x\rangle\langle\Psi_L^x|) \\ &= \frac{\chi_{A,A} + \chi_{B,B}}{2} + \frac{g_A^* g_B \chi_{A,B} + g_A g_B^* \chi_{B,A}}{2}. \end{aligned} \quad (8)$$

Both $\chi_{A,A}$ and $\chi_{B,B}$ are known from the error statistics obtained without pre-processing. Eq. (8) shows that preprocessing the quantum register with $U(a, b)$ alters the syndrome statistics in a manner that reveals the off-diagonal terms of the process matrix. Repeated measurement of stabilizers followed by error correction repeated sufficient number of times would determine the off-diagonal terms of the process matrix χ as detailed in [3]. When $[F_a, F_b] = 0$, we have $U(a, b) = (F_a + iF_b)/\sqrt{2}$ and in place of Eq. (8) we obtain:

$$\xi(a, b, x) = \frac{1}{2}(\chi_{A,A} + \chi_{B,B} + i[g_A g_B^* \chi_{B,A} - g_A^* g_B \chi_{A,B}]). \quad (9)$$

3. Toggling

Depending on the Pauli factors g_A and g_b appearing in Eqs. (8) and (9) either the real or imaginary parts

of each of the off-diagonal terms of χ would remain undetermined [3]. We can solve this problem by further pre-processing the noisy state prior to the application of $U(a, b)$ with the operator $T^+ = T \oplus I'$. In T^+ , the operator

$$T \equiv \sum_{m=0}^{d^2-1} e^{i\theta_m} \Pi_L^m, \quad (10)$$

acts on all the states within the error ball of the QEC code with Π_L^m being the projectors on to the erroneous logical space given by $F_m \Pi_C F_m$, where Π_C is the set of all codewords of the QEC scheme. The unit operator I' acts on the space of states lying outside the error ball. The angles θ_m are chosen from the set $\{\pm\pi/4\}$, with equal number of entries of each sign appearing in T . As shown in [3] this ‘toggling’ operation interchanges the real and imaginary parts of $\chi_{l,m}$ prior to U , depending on the choice of values of θ_l and θ_m . The error correction capability of the QEC code is not affected by the application of the toggling operation T^+ . In practical terms, T^+ represents 2^k copies of the usual T -gates,

$$T = \frac{1}{\sqrt{2}} \begin{pmatrix} 1+i & 0 \\ 0 & 1-i \end{pmatrix}.$$

in the l - m subspace of the error ball of each codeword. After identifying the real or imaginary parts of $\chi_{l,m}$ that were not determined by the application of $U(a, b)$, suitable toggling operations can be inserted prior to the application of the unitary so as to exchange the real and imaginary parts of the $\chi_{l,m}$'s of interest and the same procedure followed earlier can be used to estimate these as well.

With one experimental configuration i.e., preprocessing the quantum register with a $U(a, b)$ and followed by stabilizer measurements one can determine $d^2/2$ off-diagonal elements out of the $(d^4 - 2d^2 + 1)/2$ real parameters to be estimated. Thus $(d^4 - 2d^2 + 1)/d^2$ configurations are needed to obtain all the off-diagonal elements of χ and the total number of configurations needed to completely characterize χ becomes $2(d^2 - 1)$.

III. TWO-QUBIT AMPLITUDE DAMPING (2AD) ERROR MODEL

The open quantum system we focus on consists of two qubits formed by a pair of atoms with two addressable and distinct levels of interest. The energy gap between the levels $|g_j\rangle$ ($j = 1, 2$) and the corresponding ‘excited state’ $|e_j\rangle$ is $\hbar\omega_j$. Each atom has a dipole moment $\vec{\mu}_j$ and they are respectively located at \vec{r}_j with the inter-atomic separation given by $r_{12} = |\vec{r}_1 - \vec{r}_2|$. The two atoms are sitting in a bath of electromagnetic radiation which forms the environment of the open system. The interaction between the qubits and the bath is position dependent and it depends on the dipole moments of the atoms as

well. The Hamiltonian for the system, employing the dipole approximation for the qubit bath interaction is [10]

$$\begin{aligned} H &= H_S + H_B + H_{SR} \\ &= \frac{1}{2} \sum_{j=1,2} \hbar\omega_j Z_j + \sum_{\vec{k},s} \hbar\omega_k (b_{\vec{k}s}^\dagger b_{\vec{k}s} + 1/2) \\ &\quad - i\hbar \sum_{ks} \sum_{j=1,2} \vec{\mu}_i \cdot \vec{g}_{\vec{k}s}(\vec{r}_j) (S_j^+ + S_j^-) b_{\vec{k}s} - h.c. \end{aligned} \quad (11)$$

where $S_j^\pm = (X_j + iY_j)/2$ are the rising and lowering operators on j^{th} qubit, $b_{\vec{k}s}$ is the annihilation operator corresponding to a bath mode $\vec{k}s$, with wave vector \vec{k} , frequency ω_k and polarization index $s = 1, 2$. Here we are labelling the three Pauli operators on each of the qubits as X_j , Y_j and Z_j respectively. The system-bath coupling has the form

$$\vec{g}_{\vec{k}s}(\vec{r}_j) = \sqrt{\frac{\omega_k}{2\epsilon\hbar V}} \vec{\epsilon}_{\vec{k}s} e^{i\vec{k}\cdot\vec{r}_j}, \quad (12)$$

which is also the mode function of the bath evaluated at position \vec{r}_j of the j^{th} qubit and $\vec{\epsilon}_{\vec{k}s}$ is the unit polarization vector of the bath mode with V as the normalization volume.

This model was analyzed in detail in [10] where using the Born-Markov and rotating wave approximations, the following master equation is obtained for the density matrix of the two qubit system when it is interacting with a zero temperature electromagnetic bath with no squeezing:

$$\begin{aligned} \frac{d\rho}{dt} &= -\frac{i}{\hbar} [H_D, \rho] \\ &\quad - \frac{1}{2} \sum_{j,k=1}^2 \Gamma_{jk} (\rho S_j^+ S_k^- + S_j^+ S_k^- \rho - 2S_j^- \rho S_j^+), \end{aligned} \quad (13)$$

where

$$H_D = \frac{1}{2} \sum_{i=1,2} \hbar\omega_i Z_i + \hbar \sum_{j \neq k} \Omega_{jk} S_j^+ S_k^-. \quad (14)$$

It is convenient to express the reduced density matrix of the system in the ‘dressed state’ basis which is the eigenbasis of the Hamiltonian H_D given above. When the two qubits are identical, the dressed state basis is given by:

$$\begin{aligned} |g\rangle &= |g_1\rangle|g_2\rangle, & |s\rangle &= \frac{1}{\sqrt{2}}(|e_1\rangle|g_2\rangle + |g_1\rangle|e_2\rangle), \\ |e\rangle &= |e_1\rangle|e_2\rangle, & |a\rangle &= \frac{1}{\sqrt{2}}(|e_1\rangle|g_2\rangle - |g_1\rangle|e_2\rangle). \end{aligned} \quad (15)$$

with the corresponding eigenvalues being $E_g = -\hbar\omega_0$, $E_s = \hbar\Omega_{12}$, $E_a = -\hbar\Omega_{12}$ and $E_e = \hbar\omega_0$.

The Hamiltonian H_D describes the dynamics in the presence of the vacuum induced coherent dipole-dipole interaction between the two qubits. The strength of this

interaction is given by Ω_{jk} . For the two qubit case, we have

$$\Omega_{12} = \Omega_{21} = \frac{3}{4}\sqrt{\Gamma_{11}\Gamma_{22}}\mathcal{G}(r_{12}), \quad (16)$$

with

$$\begin{aligned} \mathcal{G}(r_{12}) = & -[1 - (\hat{\mu} \cdot \hat{r}_{12})^2] \frac{\cos(k_0 r_{12})}{k_0 r_{12}} \\ & + [1 - 3(\hat{\mu} \cdot \hat{r}_{12})^2] \left[\frac{\sin(k_0 r_{12})}{(k_0 r_{12})^2} + \frac{\cos(k_0 r_{12})}{(k_0 r_{12})^3} \right], \end{aligned}$$

where $\hat{\mu} = \hat{\mu}_1 = \hat{\mu}_2$ is the unit vector along the electric dipole moment of the atomic qubits which are assumed to be aligned parallel to each other and \hat{r}_{12} is the unit vector along the line joining the two qubits. The Ω_{12} term in H_D is responsible for coherently driving the excited state population between the two atomic qubits. The Γ_{jj} appearing in Eq. (16), are the spontaneous emission rates of each of the qubits due to their independent dissipative interactions with the bath and these rates are given by

$$\Gamma_{jj} = \frac{\omega_j^3 \mu_j^2}{3\pi\epsilon\hbar c^3}.$$

For the identical qubit case, $\Gamma_{11} = \Gamma_{22} = \Gamma$.

The coefficients Γ_{jk} for $j \neq k$, appearing in the master equation (13) represent collective, incoherent dissipation rates due to the system bath interaction. For the two qubit system we have

$$\Gamma_{12} = \Gamma_{21} = \frac{3}{2}\sqrt{\Gamma_{11}\Gamma_{22}}\mathcal{F}(r_{12}) = \frac{3}{2}\Gamma\mathcal{F}(r_{12}), \quad (17)$$

where

$$\begin{aligned} \mathcal{F}(r_{12}) = & [1 - (\hat{\mu} \cdot \hat{r}_{12})^2] \frac{\sin(k_0 r_{12})}{k_0 r_{12}} \\ & + [1 - 3(\hat{\mu} \cdot \hat{r}_{12})^2] \left[\frac{\cos(k_0 r_{12})}{(k_0 r_{12})^2} - \frac{\sin(k_0 r_{12})}{(k_0 r_{12})^3} \right]. \end{aligned}$$

The functions $\mathcal{G}(r_{12})$ and $\mathcal{F}(r_{12})$ represent the spatial dependence of the coherent and incoherent interactions between the qubits mediated by the bath. The wavelength, $\lambda_0 = 2\pi/k_0$ corresponding to the wave number k_0 appearing in the expressions for $\mathcal{G}(r_{12})$ and $\mathcal{F}(r_{12})$ sets the length scale for such interactions between the two qubits. Note that k_0 is also equal to ω_0/c where $\omega_0 = (\omega_1 + \omega_2)/2$ and hence λ_0 is the resonance wavelength of the qubits when they are identical. The two functions are plotted in Fig. 1

From Fig. 1 we see that as the separation between the qubits $k_0 r_{12} \rightarrow 0$ the functions \mathcal{F} and \mathcal{G} increase. The bath mediated coherent dynamics governed by Ω_{12} as well as the collective decoherence rate given by Γ_{12} both become comparable to the independent dynamics of the qubits and we obtain a collective decoherence model with predominantly correlated errors. On the other hand $k_0 r_{12} \gg 1$ we have an independent decoherence model

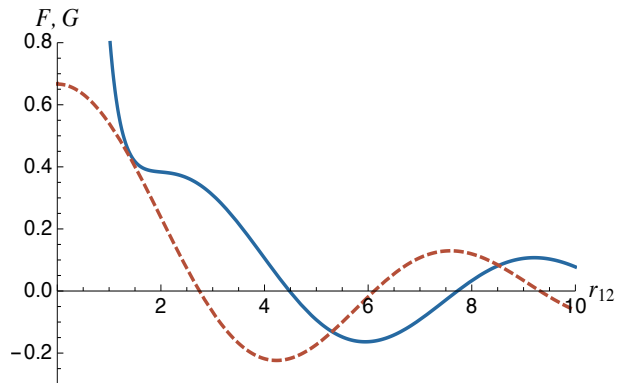


FIG. 1: The functions $\mathcal{F}(r_{12})$ (dashed, red line) and $\mathcal{G}(r_{12})$ (blue line) are plotted as a function of the separation between the qubits in arbitrary units when the dipole moments of both qubits are aligned perpendicular to the line joining the two and with $k_0 = 1$.

with the errors due to the influence of the bath on each qubit being acting independent of each other.

We assume that the initial state of the system and environment is a product state so as to ensure completely positive reduced dynamics. Let the initial state of the environment be the vacuum and that of the two-qubit system in the dressed state basis be

$$\rho = \begin{pmatrix} \rho_{ee} & \rho_{es} & \rho_{ea} & \rho_{eg} \\ \rho_{se} & \rho_{ss} & \rho_{sa} & \rho_{sg} \\ \rho_{ae} & \rho_{as} & \rho_{aa} & \rho_{ag} \\ \rho_{ge} & \rho_{gs} & \rho_{ga} & \rho_{gg} \end{pmatrix}. \quad (18)$$

After the pair of qubits and its environment has interacted for a duration t , the time evolved reduced state of the system is given by [11]

$$\begin{aligned} \rho_{\mathcal{E}} = \mathcal{E}^{2\text{AD}}(\rho) = & \\ & \begin{pmatrix} A\rho_{ee} & J\rho_{es} & M\rho_{ea} & L\rho_{eg} \\ J^*\rho_{se} & B\rho_{ss} + C\rho_{ee} & P\rho_{sa} & T\rho_{sg} + U\rho_{es} \\ M^*\rho_{ae} & P^*\rho_{as} & D\rho_{aa} + E\rho_{ee} & Q\rho_{ag} + V\rho_{ea} \\ L^*\rho_{ge} & T^*\rho_{gs} + U^*\rho_{se} & Q^*\rho_{ga} + V^*\rho_{ae} & \rho_{gg} + F\rho_{ss} + G\rho_{aa} + H\rho_{ee} \end{pmatrix}, \end{aligned} \quad (19)$$

where the functions A, B , etc. are given in Appendix A.

IV. CORRELATED NOISE

In the regime, $k_0 r_{12} \ll 1$, we expect the collective decoherence of the pair of qubits, whose strength is given by Γ_{12} , to produce correlated noise on the qubit pair. This would mean that the probabilities for simultaneous errors on the two qubits will not factorize: $p(x_1, x_2) \neq p(x_1)p(x_2)$. In general, a dynamical map $\mathcal{E}_{1,2,\dots,n}$ acting on n qubits as $\rho'_{1,2,\dots,n} = \mathcal{E}_{1,2,\dots,n}(\rho_{1,2,\dots,n})$ produces correlated noise. The noise is uncorrelated only if the

action of the map is independent on each qubit; i.e.,

$$\mathcal{E}_{1,2,\dots,n} = \mathcal{E}_1 \otimes \mathcal{E}_2 \otimes \dots \otimes \mathcal{E}_n. \quad (20)$$

If the initial state is in the product form $\rho_{1,2,\dots,n} = \rho_1 \otimes \rho_2 \otimes \dots \otimes \rho_n$, noise of the type in Eq. (20) will preserve the product form. Any departure of $\mathcal{E}_{1,2,\dots,n}(\rho_{1,2,\dots,n})$ from the product form leads to correlated noise which in turn will give rise to nonclassical correlations in quantum states $\rho_{1,2,\dots,n}$ characterized by quantum discord. For the two qubit case, the noise is uncorrelated if we can write the process matrix in the form

$$\mathcal{E}(\rho) = \sum_{jk,lm} \chi_{jk\chi lm} (F_j \otimes F_l) \rho (F_k \otimes F_m), \quad (21)$$

From Eq. (21) we see that for uncorrelated noise, the process matrix χ has the product form $\chi_1 \otimes \chi_2$.

We can quantify the degree of correlation in the noise on the two qubit system by defining a measure for the same as

$$\mathcal{D} = \|\chi - (\chi_1 \otimes \chi_2)\|, \quad (22)$$

where $\|\cdot\|$ denotes an appropriate distance measure in the space of two qubit process matrices χ . Since the process matrices are normal, we can use the trace distance as an appropriate distance measure [2]. The trace distance between two normal matrices ρ_A and ρ_B is defined as

$$\|\rho_A - \rho_B\| \equiv \frac{1}{2} \sqrt{(\rho_A - \rho_B)^\dagger (\rho_A - \rho_B)} = \frac{1}{2} \sum_{j=1}^d |\lambda_j|,$$

where λ_j are the eigenvalues (not necessarily real or positive) of the normal matrix $\rho_A - \rho_B$.

Note that any other suitable measure of distance or distinguishability that captures the above idea would also work, for example, quantum mutual information defined via quantum relative entropy:

$$\begin{aligned} \mathcal{D}^* &\equiv S(\rho_{AB} || \rho_A \otimes \rho_B) \\ &= S(\rho_A) + S(\rho_B) - S(\rho_{AB}), \end{aligned} \quad (23)$$

where $S(\cdot)$ is von Neumann entropy and $S(\cdot || \cdot)$ is quantum relative entropy. The quantity \mathcal{D}^* vanishes precisely if ρ_{AB} has the product form. In general, $S(\rho_1 || \rho_2)$ may diverge, which would happen if there is a non-vanishing overlap between the support of ρ_1 and the kernel of ρ_2 . For \mathcal{D}^* , this problem does not arise because the two arguments in the definition have identical support.

V. CHARACTERIZATION OF \mathcal{E}^{2AD} VIA 5-QUBIT QECCD

We use the the [[5, 1]] QEC code introduced in Ref. [3], with two logical basis states,

$$\begin{aligned} |0_L\rangle &= \frac{1}{2\sqrt{2}} (|00000\rangle + |00110\rangle + |01001\rangle - |01111\rangle \\ &\quad - |10011\rangle + |10101\rangle + |11010\rangle + |11100\rangle) \\ |1_L\rangle &= XXXXX|0_L\rangle, \end{aligned} \quad (24)$$

to reconstruct \mathcal{E}^{2AD} using QECCD. The code is capable of correcting arbitrary errors on the first two qubits which we consider as the primary system \mathbf{P} . The QEC code states are represented in the computational basis and the stabilizers generators of the code are the mutually commuting operators, $IZZZZ$, $XXXII$, $ZXZIX$, and $ZZXXI$. An arbitrary logical state of the QEC code has the form

$$|\Psi_L\rangle = \beta_0|0_L\rangle + \beta_1|1_L\rangle, \quad |\beta_0|^2 + |\beta_1|^2 = 1. \quad (25)$$

The register of five qubits is initialized in a logical state as given in Eq. (25) and the primary system \mathbf{P} is subjected to \mathcal{E}^{2AD} noise, while the remaining three ancilla qubits are assumed to be noise free. The initial and final states of the five qubit register are therefore given by

$$\rho_c = |\Psi_L\rangle\langle\Psi_L|, \quad \text{and} \quad \rho_c^{2AD} = (\mathcal{E}^{2AD} \otimes I^{\otimes 3}) \rho_c,$$

respectively. The sixteen operators corresponding to strings of length two taken from the set $\{I, X, Y, Z\} \otimes \{I, X, Y, Z\}$ form the error basis and the corresponding syndromes obtained through measurements of the stabilizers are given in Table I. Fig. 2 shows the quantum circuit to implement the stabilizer measurement for the 5-qubit QEC code in Eq. (24) using only one and two qubit interactions [30].

Error	II	XI	YI	ZI	IX	IY	IZ	XX
IZZZZ	+	+	+	+	-	-	+	-
XXXII	+	+	-	-	+	-	-	+
ZXZIX	+	-	-	+	+	-	-	-
ZZXXI	+	-	-	+	-	-	+	+
Error	XY	XZ	YX	YY	YZ	ZX	ZY	ZZ
IZZZZ	-	+	-	-	+	-	-	+
XXXII	-	-	-	+	+	-	+	+
ZXZIX	+	+	-	+	+	+	-	-
ZZXXI	+	-	+	+	-	-	+	+

TABLE I: The error syndromes (patterns of measurement outcomes of the stabilizer operators) corresponding to errors on \mathbf{P} . "+" represents +1 measurement out come upon the measurement of stabilizer S_j on ρ_c^{2AD} , while the "-" stands for measurement out come being -1.

A. Diagonal terms of χ^{2AD}

As mentioned in Sec. II A 1 one can measure all the diagonal terms of the χ matrix in a single apparatus configuration since all the stabilizers commute with each other. Knowing the error model and using Eq. (19) that gives the time evolution of the system \mathbf{P} , we can compute the expected statistics for obtaining each of the syndromes in Table. I. This in turn gives the diagonal elements of the process matrix of the channel \mathcal{E}^{2AD} as in Eq. (6).

Equations. (18) and (19) give the states of \mathbf{P} before and after the action of the noise. The Ref. [16] provides

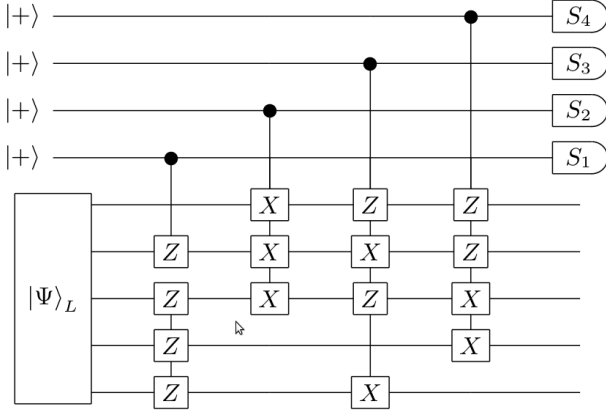


FIG. 2: Circuit to measure the stabilizer generators for our 5-qubit code using only one and two qubit interaction. The first four inputs to the circuit are the ancilla qubits in the state $|+\rangle = \frac{|0\rangle+|1\rangle}{\sqrt{2}}$. The last five input qubits correspond to the QEC code initialized in the state $|\Psi\rangle_L$. The boxes represent the controlled operations (X, Y, Z) with the control being the filled circle at the other end of the wire. The boxes S_j represent measurement in the computational basis.

the operator sum-difference representation of \mathcal{E}^{2AD} with Kraus-like operators \mathcal{K}_j^\pm according to which the action of the noise on the \mathbf{P} of $|\Psi_L\rangle$ is

$$\rho_c^{2AD} = \sum_j (\mathcal{K}_j^+ \otimes \mathbb{1}_2^{\otimes 3}) \rho_c (\mathcal{K}_j^+ \otimes \mathbb{1}_2^{\otimes 3})^\dagger - (\mathcal{K}_j^- \otimes \mathbb{1}_2^{\otimes 3}) \rho_c (\mathcal{K}_j^- \otimes \mathbb{1}_2^{\otimes 3})^\dagger, \quad (26)$$

where $\mathbb{1}_2$ is identity on qubit. Before applying the \mathcal{E}^{2AD} , \mathbf{P} is transformed to the dressed state basis using the unitary $U_D \otimes \mathbb{1}^{\otimes 3}$, where

$$U_D = \begin{pmatrix} 1 & 0 & 0 & 0 \\ 0 & 1/\sqrt{2} & 1/\sqrt{2} & 0 \\ 0 & 1/\sqrt{2} & -1/\sqrt{2} & 0 \\ 0 & 0 & 0 & 1 \end{pmatrix},$$

and back to $\{0,1\}$ basis after application of \mathcal{E}^{2AD} using $(U_D \otimes \mathbb{1}^{\otimes 3})^{-1}$. Alternatively, by inspection, one can write down the map corresponding to the noise in the matrix super-operator from of Eq. (1). The matrix \mathcal{A} corresponding to the \mathcal{E}^{2AD} is a 16×16 sparse matrix with the following entries in the diagonal:

$$(A, J, M, L, J^*, B, P, T, M^*, P^*, D, Q, L^*, T^*, Q^*, 1),$$

where $A, B \dots$ are given in Appendix A. The remaining non-zero elements of \mathcal{A} are $\mathcal{A}_{6,1} = C$, $\mathcal{A}_{8,2} = U$, $\mathcal{A}_{11,1} = E$, $\mathcal{A}_{12,3} = V$, $\mathcal{A}_{14,5} = U^*$, $\mathcal{A}_{15,9} = V^*$, $\mathcal{A}_{16,1} = H$, $\mathcal{A}_{16,6} = F$ and $\mathcal{A}_{16,11} = G$. After transforming the initial logical state from Eq. (25) into the dressed state basis using the unitary $U_D \otimes \mathbb{1}^{\otimes 3}$, we can apply the map $\mathcal{A} \otimes \mathbb{1}_4^{\otimes 3}$ on the vectorized form of $|\Psi_L\rangle\langle\Psi_L|$. Here $\mathbb{1}_4$ in the identity super-operator on each of the vectorized ancilla

qubits. Reshuffling the result back into a density matrix we get the state of the register after the action of the noise which can be expanded in the error basis as

$$\rho_c^{2AD} = \sum_{lm}^{d^2-1} \chi_{l,m} |\Psi_L^l\rangle\langle\Psi_L^m|.$$

Using Eq. (6), the diagonal elements of χ^{2AD} are obtained as

$$\chi_{II,II} = \frac{1}{16} [1 + A + B + D + 2(\text{Re}(J) + \text{Re}(L) + \text{Re}(M) + \text{Re}(P) + \text{Re}(Q) + \text{Re}(T))],$$

$$\begin{aligned} \chi_{XI,XI} &= \chi_{IX,IX} = \chi_{YZ,YZ} = \chi_{ZY,ZY} \\ &= \frac{1}{32} [C + E + F + G + 2(\text{Re}(U) - \text{Re}(V))], \end{aligned}$$

$$\begin{aligned} \chi_{YI,YI} &= \chi_{IY,IY} = \chi_{XZ,XZ} = \chi_{ZX,ZX} \\ &= \frac{1}{32} [C + E + F + G - 2(\text{Re}(U) - \text{Re}(V))], \end{aligned}$$

$$\chi_{ZI,ZI} = \chi_{IZ,IZ} = \frac{1}{16} [1 + A - 2\text{Re}(L)],$$

$$\chi_{XX,XX} = \chi_{YY,YY} = \frac{1}{16} [B + D + H - 2\text{Re}(P)],$$

$$\chi_{XY,XY} = \chi_{YX,YX} = \frac{1}{16} H,$$

$$\begin{aligned} \chi_{ZZ,ZZ} &= \frac{1}{16} [1 + A + B + D - 2(\text{Re}(J) - \text{Re}(L) \\ &\quad + \text{Re}(M) - \text{Re}(P) + \text{Re}(Q) - \text{Re}(T))]. \end{aligned}$$

The noise is symmetric on the two qubits i.e., action of the noise under the change of the label of the qubits is invariant. This is reflected in the fact that under the interchange of the qubit-label the equations above remain the same.

B. Off-diagonal terms of χ^{2AD}

To find the off-diagonal terms of χ^{2AD} using QECCD as described in Sec. II A 2, we have to pre-process the state ρ_c^{2AD} with unitaries $U(a,b)$ described in Eq. (7) with suitable a and b chosen from the error basis. These will however yield only either the real or imaginary part of the off-diagonal terms of the process matrix. To obtain the other missing part, we will have to do an additional toggling operation that exchanges the real and imaginary parts of χ^{2AD} . The necessary toggling operators are constructed following the heuristic described in the Sec. II A 3.

To determine the real/imaginary part of $\chi_{l,m}$ not possible by applying $U(a,b)$, place equal number of the l^{th}

and the m^{th} error elements in the opposite partitions created by the coefficients $(1+i)$ and $(1-i)$ as

$$T^+ = \frac{1}{\sqrt{2}} \left[(1+i) \sum_l F_l \rho_c F_l + (1-i) \sum_m F_m \rho_c F_m \right]. \quad (27)$$

For example to toggle the elements in the table corresponding to $U(II,IZ)$ in Appendix B, place the elements $II, IX, XI, XX, IY, YX, IZ, ZX$ and $IZ, IY, XZ, XY, YZ, YY, ZZ, ZY$ in the different partitions i.e.,

$$\begin{aligned} T_1^+ &= \frac{1+i}{\sqrt{2}} (\rho_c + IX\rho_c IX + XI\rho_c XI + XX\rho_c XX \\ &\quad + YI\rho_c YI + YX\rho_c YX + ZI\rho_c ZI + ZX\rho_c ZX) \\ &\quad + \frac{1-i}{\sqrt{2}} (IZ\rho_c IZ + IY\rho_c IY + XZ\rho_c XZ \\ &\quad + XY\rho_c XY + YZ\rho_c YZ + YY\rho_c YY \\ &\quad + ZZ\rho_c ZZ + ZY\rho_c ZY). \end{aligned}$$

Similarly, other operators T_2^+, \dots, T_7^+ can be constructed.

The tables in Appendix B list the necessary unitary and toggling operations as well as the syndrome measurements that are to be performed to obtain both real and imaginary parts of all the non-zero off-diagonal terms of the process matrix $\chi^{2\text{AD}}$.

Further, in the independent regime, $r_{12}/\lambda_0 \gg 1$ the quantities $A, B, C, D, E, J, L, M, P, Q, T, U$ and V all

go to zero when $t \rightarrow \infty$, where as F, G , and H become equal to 1. All the diagonal and off-diagonal terms of the process matrix $\chi^{2\text{AD}}$ reach the value $1/16$ asymptotically and the matrix factors out as follows

$$\text{ind } \chi_{\text{asy}}^{2\text{AD}} = \frac{1}{16} \begin{pmatrix} 1 & 0 & 0 & -1 \\ 0 & 1 & i & 0 \\ 0 & -i & 1 & 0 \\ -1 & 0 & 0 & 1 \end{pmatrix} \otimes \begin{pmatrix} 1 & 0 & 0 & -1 \\ 0 & 1 & i & 0 \\ 0 & -i & 1 & 0 \\ -1 & 0 & 0 & 1 \end{pmatrix}. \quad (28)$$

In the collective regime where $r_{12}/\lambda_0 \rightarrow 0$, from Eq. (17) we see that $\Gamma_{12} = \Gamma_{21} = \Gamma$ since $\mathcal{F}(0) = 2/3$. Then we see that $A, B, C, E, J, L, M, P, T, U$, and V go to zero as $t \rightarrow \infty$. At the same time we have D, F, G , and H going to 1 while $Q \rightarrow e^{-i(\omega_0 - \Omega_{12})t}$. This means that

$$\chi_{II,II} = \chi_{ZZ,ZZ} = \frac{2 + \cos(\omega_0 - \Omega_{12})}{16},$$

are oscillatory functions in the collective regime with a frequency $\omega_0 - \Omega_{12}$. Note that the function \mathcal{G} in Eq. (16) goes to infinity when $r_{12}/\lambda_0 \rightarrow 0$. So $\chi_{II,II}$ and $\chi_{ZZ,ZZ}$ are rapidly oscillating functions of time when r_{12} is small. When the two qubits are very close together, we can average over the rapid oscillations and then $\chi_{II,II}$ and $\chi_{ZZ,ZZ}$ take on the limiting value of $1/8$ along with the diagonal terms $\chi_{YZ,YZ}$ and $\chi_{XY,XY}$. The terms χ_{Z_2,Z_2} , $\chi_{XY,XY}$ and $\chi_{YY,YY}$ become $1/8$ while rest of the diagonal terms go to $1/32$ as $t \rightarrow \infty$ and the process matrix has non-factorizable asymptotic form:

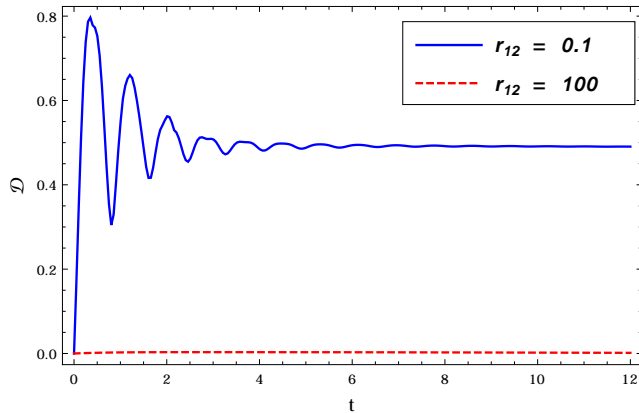
$$\text{col } \chi_{\text{asy}}^{2\text{AD}} = \frac{1}{32} \begin{pmatrix} 4 & 0 & 0 & -2 & 0 & -2 & 0 & 0 & 0 & 0 & -2 & 0 & -2 & 0 & 0 & 0 \\ 0 & 1 & i & 0 & 1 & 0 & 0 & -1 & i & 0 & 0 & -i & 0 & -1 & -i & 0 \\ 0 & -i & 1 & 0 & -i & 0 & 0 & i & 1 & 0 & 0 & -1 & 0 & i & -1 & 0 \\ -2 & 0 & 0 & 2 & 0 & 0 & 0 & 0 & 0 & 0 & 0 & 0 & 2 & 0 & 0 & -2 \\ 0 & 1 & i & 0 & 1 & 0 & 0 & -1 & i & 0 & 0 & -i & 0 & -1 & -i & 0 \\ -2 & 0 & 0 & 0 & 0 & 4 & 2i & 0 & 0 & 2i & 0 & 0 & 0 & 0 & 0 & 2 \\ 0 & 0 & 0 & 0 & 0 & -2i & 2 & 0 & 0 & 2 & 2i & 0 & 0 & 0 & 0 & 0 \\ 0 & -1 & -i & 0 & -1 & 0 & 0 & 1 & -i & 0 & 0 & i & 0 & 1 & i & 0 \\ 0 & -i & 1 & 0 & -i & 0 & 0 & i & 1 & 0 & 0 & -1 & 0 & i & -1 & 0 \\ 0 & 0 & 0 & 0 & 0 & -2i & 2 & 0 & 0 & 2 & 2i & 0 & 0 & 0 & 0 & 0 \\ -2 & 0 & 0 & 0 & 0 & 0 & -2i & 0 & 0 & -2i & 4 & 0 & 0 & 0 & 0 & 2 \\ 0 & i & -1 & 0 & i & 0 & 0 & -i & -1 & 0 & 0 & 1 & 0 & -i & 1 & 0 \\ -2 & 0 & 0 & 2 & 0 & 0 & 0 & 0 & 0 & 0 & 0 & 0 & 2 & 0 & 0 & -2 \\ 0 & -1 & -i & 0 & -1 & 0 & 0 & 1 & -i & 0 & 0 & i & 0 & 1 & i & 0 \\ 0 & i & -1 & 0 & i & 0 & 0 & -i & -1 & 0 & 0 & 1 & 0 & -i & 1 & 0 \\ 0 & 0 & 0 & -2 & 0 & 2 & 0 & 0 & 0 & 0 & 2 & 0 & -2 & 0 & 0 & 4 \end{pmatrix} \quad (29)$$

C. Noise correlation in the 2AD channel

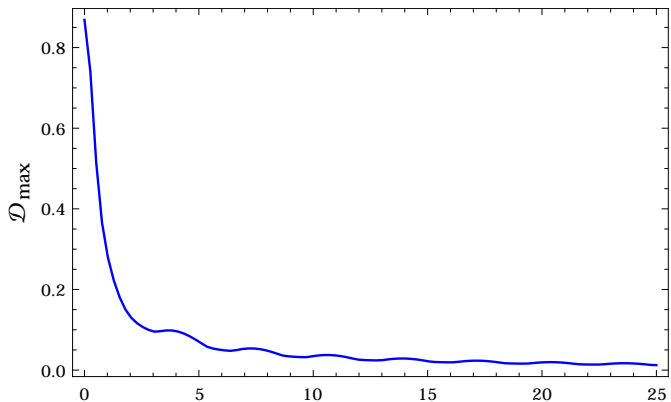
Since the coefficients A, B , etc. that appear in Eq. (19) are time dependent, the dynamical map $\mathcal{E}^{2\text{AD}}$ and the corresponding process matrix also have time dependence.

In Fig. 3(a), the time dependence of the measure of correlation in the noise, \mathcal{D} is plotted for the cases where the two qubits are close by with $r_{12} = 0.1$ in units of λ_0 and where the two are far apart with $r_{12} = 100$. We see that when the two qubits are close to each other the measure

of correlation in the noise is finite indicating that the coherent as well as incoherent couplings between the two qubits mediated by the bath leads to correlated errors on the two qubits. When r_{12} is large, the measure of correlation is identically zero at all times. In Fig. 3(b), the maximum of \mathcal{D} as a function of time is plotted against the inter qubit separation r_{12} . We again see that, as expected, when the separation increases, the degree of correlation in the $\mathcal{E}^{2\text{AD}}$ noise decreases.



(a)



(b)

FIG. 3: (a) \mathcal{D} of Eq.(22) plotted against t both in the collective regime (solid curve, $r_{12} = 0.1$) and the independent regime (dashed curve, $r_{12} = 100$). In the independent regime, there is no correlation between the noise acting on the two qubits. (b) \mathcal{D}_{max} is the value of \mathcal{D} maximized over t for each r_{12} is plotted as a function of r_{12} . We see that for large values of the inter-qubit separation, the correlation in the noise approaches zero. The values assigned to the bath parameters are $\gamma_0 = 0.5$, $\omega_0 = 1$ and $k_0 = 1$ in the units where $\hbar = 1$.

In view of Figure 3(b), sufficient far-spaced qubits subjected to the 2AD noise will fail to produce any quantum correlation when start in a product state. However, as the collective-noise regime is approached, qubits start in

a product can have non-classical correlation characterized by quantum discord under the $\mathcal{E}^{2\text{AD}}$ noise.

The correlated noise can generate non-classical corre-

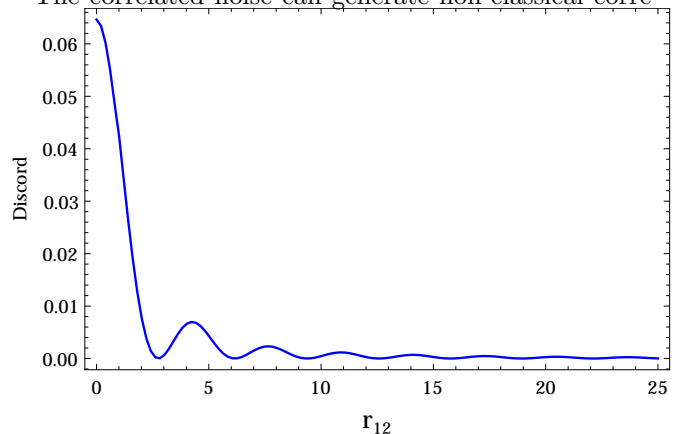


FIG. 4: The discord maximized over t for each r_{12} is plotted as a function of r_{12} . We see that for large values of the inter-qubit separation, the discord approaches zero, in accordance with the asymptotically vanishing \mathcal{D}_{max} in Fig. 3(b). The values assigned to the bath parameters are $\gamma_0 = 0.5$, $\omega_0 = 1$ and $k_0 = 1$ in the units where $\hbar = 1$.

lations between the qubits as characterized by quantum discord even if the qubits are in an initial product state. In the case of $\mathcal{E}^{2\text{AD}}$, as the inter-qubit distance is increased the correlation in the noise decreases resulting in the decrease of quantum discord generated. Fig. 4 shows the quantum discord as defined in Ref. [31] in a two-qubit system (starting in the product state $|0\rangle \otimes |0\rangle$) evolving under $\mathcal{E}^{2\text{AD}}$ as a function of inter-qubit distance r_{12} . The value of quantum discord approaches zero as the correlation in the $\mathcal{E}^{2\text{AD}}$ goes to zero.

VI. DISCUSSION AND CONCLUSION

In this work, we studied the dependence of the 2AD (2-qubit amplitude damping) channel on inter-qubit separation, showing in particular that it becomes completely uncorrelated in the independent limit, but retains strong correlation in the collective limit. Correlatedness of the noise is quantified in terms of the departure of the process matrix from the product form. Further, we presented a detailed QECCD protocol to completely characterize 2AD noise. The protocol can be easily extended for the characterization of both dissipative [11] and non-dissipative [32] dynamics due to squeezed-thermal bath, replacing the vacuum bath.

The protocol can be physically implemented on NMR systems[33], linear optics with post selection [34] and superconducting qubit system [35] that are used for achieving fault tolerant quantum computation.

- [1] D. A. Lidar and T. Brun, *Quantum Error Correction* (Cambridge University Press, 2013).
- [2] M. Nielsen and I. Chuang, *Quantum Computation and Quantum Information* (Cambridge University Press (Cambridge), 2000).
- [3] S. Omkar, R. Srikanth, and S. Banerjee, Phys. Rev. A **91**, 012324 (2015).
- [4] W. G. Unruh, Phys. Rev. A **51**, 992 (1995).
- [5] E. Knill, R. Laflamme, and W. H. Zurek, Science **279**, 342 (1998).
- [6] N. Boulant, T. F. Havel, M. A. Pravia, and D. G. Cory, Phys. Rev. A **67**, 042322 (2003).
- [7] R. Laflamme et al., Phys. Rev. Lett. **77**, 198 (1996).
- [8] G. Chiribella, M. Dall'Arno, G. M. D'Ariano, C. Macchiavello, and P. Perinotti, Phys. Rev. A **83**, 052305 (2011).
- [9] C.-K. Li, M. Nakahara, Y.-T. Poon, N.-S. Sze, and H. Tomita, Physics Letters A **375**, 3255 (2011), ISSN 0375-9601.
- [10] Z. Ficek and R. Tanaś, Phys. Rep. **372**, 369 (2002).
- [11] S. Banerjee, V. Ravishankar, and R. Srikanth, Ann. of Phys. **325**, 816 (2010).
- [12] L. Henderson and V. Vedral, J. Phys. A: Math. Gen. **34**, 6899 (2001).
- [13] H. Ollivier and W. Zurek, Phys. Rev. Lett. **88**, 017901 (2001).
- [14] E. C. G. Sudarshan, P. M. Mathews, and J. Rau, Phys. Rev. **121**, 920 (1961).
- [15] K. Kraus, *States, Effects and Operations: Fundamental Notions of Quantum Theory*, vol. 190 of *Lecture notes in Physics* (Spring-Verlag, New York, 1983).
- [16] S. Omkar, R. Srikanth, and S. Banerjee, Quantum Information Processing pp. 1–15 (2015), ISSN 1570-0755.
- [17] G. M. D'Ariano, Fortschritte der Physik **48**, 579 (2000).
- [18] G. M. D'Ariano and P. Lo Presti, Phys. Rev. Lett. **86**, 4195 (2001).
- [19] J. B. Altepeter et al., Phys. Rev. Lett. **90**, 193601 (2003).
- [20] G. M. D'Ariano, Phys. Lett. A **300**, 1 (2002).
- [21] M. Mohseni and D. A. Lidar, Phys. Rev. Lett. **97**, 170501 (2006).
- [22] M. Mohseni and D. A. Lidar, Phys. Rev. A **75**, 062331 (2007).
- [23] J. Emerson et al., Science **317**, 1893 (2007).
- [24] M. Silva, E. Magesan, D. W. Kribs, and J. Emerson, Phys. Rev. A **78**, 012347 (2008).
- [25] A. Bendersky, F. Pastawski, and J. P. Paz, Phys. Rev. Lett. **100**, 190403 (2008).
- [26] C. T. Schmiegelow, A. Bendersky, M. A. Larotonda, and J. P. Paz, Physical Review Letters **107**, 100502 (2011).
- [27] D. Gottesman (2009), arXiv:0904.2557.
- [28] S. Omkar, R. Srikanth, and S. Banerjee, Phys. Rev. A **91**, 052309 (2015).
- [29] D. Gottesman, *Stabilizer codes and quantum error correction* (1997), ph.D Thesis, arXiv:quant-ph/9705052.
- [30] M. Gupta, A. Pathak, R. Srikanth, and P. K. Panigrahi, Int. Journal of Quantum Information **5**, 627 (2007).
- [31] B. Dakić, V. Vedral, and i. c. v. Brukner, Phys. Rev. Lett. **105**, 190502 (2010).
- [32] S. Banerjee, V. Ravishankar, and R. Srikanth, The European Physical Journal D **56**, 277 (2010), ISSN 1434-6060.
- [33] A. Shukla, K. R. K. Rao, and T. S. Mahesh, Phys. Rev. A **87**, 062317 (2013).
- [34] E. Knill, R. Laflamme, and G. J. Milburn, Nature **409**, 46 (2001).
- [35] R. Barends and et.al, Nature **508**, 500 (2014).

Appendix A: The coefficients appearing in ρ_t

$$A = e^{-2\Gamma t},$$

$$B = e^{-(\Gamma+\Gamma_{12})t},$$

$$C = \frac{\Gamma + \Gamma_{12}}{\Gamma - \Gamma_{12}} [1 - e^{-(\Gamma-\Gamma_{12})t}] e^{-(\Gamma+\Gamma_{12})t},$$

$$D = e^{-(\Gamma-\Gamma_{12})t},$$

$$E = \frac{\Gamma - \Gamma_{12}}{\Gamma + \Gamma_{12}} [1 - e^{-(\Gamma+\Gamma_{12})t}] e^{-(\Gamma-\Gamma_{12})t},$$

$$F = 1 - e^{-(\Gamma+\Gamma_{12})t},$$

$$G = 1 - e^{-(\Gamma-\Gamma_{12})t},$$

$$H = \frac{\Gamma + \Gamma_{12}}{2\Gamma} \left\{ 1 - \frac{2}{\Gamma - \Gamma_{12}} \left[\frac{\Gamma + \Gamma_{12}}{2} (1 - e^{-(\Gamma-\Gamma_{12})t}) + \frac{\Gamma - \Gamma_{12}}{2} e^{-(\Gamma+\Gamma_{12})t} \right] \right\}$$

$$+ \frac{\Gamma - \Gamma_{12}}{\Gamma + \Gamma_{12}} \left\{ 1 - e^{-(\Gamma-\Gamma_{12})t} - \frac{\Gamma - \Gamma_{12}}{2\Gamma} (1 - e^{-2\Gamma t}) \right\}.$$

$$J = e^{-i(\omega_0 - \Omega_{12})t} e^{-(3\Gamma + \Gamma_{12})t/2}.$$

$$L = e^{-i2\omega_0 t} e^{-\Gamma t}.$$

$$M = e^{-i(\omega_0 + \Omega_{12})t} e^{-(3\Gamma - \Gamma_{12})t/2}.$$

$$P = e^{-i2\Omega_{12}t} e^{-\Gamma t}.$$

$$Q = e^{-i(\omega_0 - \Omega_{12})t} e^{-(\Gamma - \Gamma_{12})t/2}.$$

$$T = e^{-i(\omega_0 + \Omega_{12})t} e^{-(\Gamma + \Gamma_{12})t/2}.$$

$$U = \frac{\Gamma + \Gamma_{12}}{\Gamma^2 + 4\Omega_{12}^2} e^{-i(\omega_0 + \Omega_{12})t} e^{-(\Gamma + \Gamma_{12})t/2}$$

$$\times \left\{ 2\Omega_{12} e^{-\Gamma t} \sin(2\Omega_{12}t) + \Gamma [1 - e^{-\Gamma t} \cos(2\Omega_{12}t)] \right\}$$

$$+ i \frac{\Gamma + \Gamma_{12}}{\Gamma^2 + 4\Omega_{12}^2} e^{-i(\omega_0 + \Omega_{12})t} e^{-(\Gamma + \Gamma_{12})t/2}$$

$$\times \left\{ 2\Omega_{12} [1 - e^{-\Gamma t} \cos(2\Omega_{12}t)] - \Gamma e^{-\Gamma t} \sin(2\Omega_{12}t) \right\}.$$

$$V = i \frac{\Gamma - \Gamma_{12}}{\Gamma^2 + 4\Omega_{12}^2} e^{-i(\omega_0 - \Omega_{12})t} e^{-(\Gamma - \Gamma_{12})t/2}$$

$$\times \left\{ 2\Omega_{12} [1 - e^{-\Gamma t} \cos(2\Omega_{12}t)] - \Gamma e^{-\Gamma t} \sin(2\Omega_{12}t) \right\}$$

$$- \frac{\Gamma - \Gamma_{12}}{\Gamma^2 + 4\Omega_{12}^2} e^{-i(\omega_0 - \Omega_{12})t} e^{-(\Gamma - \Gamma_{12})t/2}$$

$$\times \left\{ 2\Omega_{12} e^{-\Gamma t} \sin(2\Omega_{12}t) + \Gamma [1 - e^{-\Gamma t} \cos(2\Omega_{12}t)] \right\}.$$

Appendix B: Protocol to characterize the 2AD channel

The tables below give the unitary operators, measurements and the toggling operators to be used to pre-process the noisy state and the syndrome statistics that are to be collected for estimating the real and imaginary parts of the off-diagonal

elements of the process matrix. In the tables below the first column indicates the unitary operator to be used, the second column indicates the syndrome to be measured and the third column lists the toggling operators (if any) to be used. The last column shows the element of χ^{2AD} that is measured along with its value.

$U(II, IZ)$	II	None	$\text{Re}(\chi_{II,IZ}) = \frac{1}{16}[A - 1 + \text{Re}(J) + \text{Re}(M) - \text{Re}(Q) - \text{Re}(T)]$
		T_1^+	$\text{Im}(\chi_{II,IZ}) = \frac{1}{16}[2 \text{Im}(L) + \text{Im}(J) + \text{Im}(M) + \text{Im}(Q) + \text{Im}(T)]$
	IX	T_1^+	$\text{Re}(\chi_{IX,IY}) = 0$
		None	$\text{Im}(\chi_{IX,IY}) = \frac{1}{32}[C + E + F + G + 2\text{Re}(U) - 2\text{Re}(V)]$
	XI	None	$\text{Re}(\chi_{XI,XZ}) = \frac{1}{32}(C + E - F - G)$
		T_1^+	$\text{Im}(\chi_{XI,XZ}) = \frac{1}{16}[\text{Im}(U) - \text{Im}(V)]$
	XX	T_1^+	$\text{Re}(\chi_{XX,XY}) = 0$
		None	$\text{Im}(\chi_{XX,XY}) = \frac{1}{16}H$
	IY	None	$\text{Re}(\chi_{IY,YZ}) = \frac{1}{32}(C + E - F - G)$
		T_1^+	$\text{Im}(\chi_{IY,YZ}) = \frac{1}{16}[\text{Im}(U) - \text{Im}(V)]$
	YX	T_1^+	$\text{Re}(\chi_{YX,YY}) = 0$
		None	$\text{Im}(\chi_{YX,YY}) = \frac{1}{16}H$
	IZ	None	$\text{Re}\chi_{IZ,ZZ} = \frac{1}{16}[A - 1 - \text{Re}(J) - \text{Re}(M) + \text{Re}(Q) + \text{Re}(T)]$
		T_1^+	$\text{Im}\chi_{IZ,ZZ} = \frac{1}{16}[\text{Im}(J) - 2\text{Im}(L) + \text{Im}(M) + \text{Im}(Q) + \text{Im}(T)]$
	ZX	T_1^+	$\text{Re}(\chi_{ZX,ZY}) = 0$
		None	$\text{Im}(\chi_{ZX,ZY}) = \frac{1}{32}[C + E + F + G - 2(\text{Re}(X) - \text{Re}(Y))]$

$U(II, ZI)$	II	None	$\text{Re}(\chi_{II,ZI}) = \frac{1}{16}[A - 1 + \text{Re}(J) + \text{Re}(M) - \text{Re}(Q) - \text{Re}(T)]$
		T_2^+	$\text{Im}(\chi_{II,ZI}) = \frac{1}{16}[2 \text{Im}(L) + \text{Im}(J) + \text{Im}(M) + \text{Im}(Q) + \text{Im}(T)]$
	IX	None	$\text{Re}(\chi_{IX,ZX}) = \frac{1}{32}(C + E - F - G)$
		T_2^+	$\text{Im}[\chi_{IX,ZX}] = \frac{1}{16}(\text{Im}(U) - \text{Im}(V))$
	XI	T_2^+	$\text{Re}(\chi_{XI,YI}) = 0$
		None	$\text{Im}(\chi_{XI,YI}) = \frac{1}{32}[C + E + F + G + 2\text{Re}(U) + 2\text{Re}(V)]$
	XX	T_2^+	$\text{Re}(\chi_{XX,YX}) = 0$
		None	$\text{Im}(\chi_{XX,YX}) = \frac{1}{16}H$
	XY	T_2^+	$\text{Re}(\chi_{XY,YY}) = 0$
		None	$\text{Im}(\chi_{XY,YY}) = \frac{1}{16}H$

$U(II, XX)$	II	None	$\text{Re}(\chi_{II,XX}) = \frac{1}{16}[B - D + \text{Re}(J) - \text{Re}(M) - \text{Re}(Q) + \text{Re}(T)]$
		T_3^+	$\text{Im}(\chi_{II,XX}) = \frac{1}{16}[2 \text{Im}(P) - \text{Im}(J) + \text{Im}(M) - \text{Im}(Q) + \text{Im}(T)]$
	IX	None	$\text{Re}(\chi_{IX,XI}) = \frac{1}{32}[C - E + F - G + 2\text{Re}(U) + 2\text{Re}(V)]$
		T_3^+	$\text{Im}(\chi_{IX,XI}) = 0$
	IY	T_3^+	$\text{Re}(\chi_{IY,XZ}) = \frac{1}{16}[\text{Re}(U) + \text{Re}(V)]$
		None	$\text{Im}(\chi_{IY,XZ}) = -\frac{1}{32}(C - E - F + G)$
	YI	T_3^+	$\text{Re}(\chi_{YI,ZX}) = \frac{1}{16}[\text{Re}(X) + \text{Re}(Y)]$
		None	$\text{Im}(\chi_{YI,ZX}) = -\frac{1}{32}(C - E - F + G)$
	YY	None	$\text{Re}(\chi_{YY,ZZ}) = -\frac{1}{16}[-B + D + \text{Re}(J) - \text{Re}(M) - \text{Re}(Q) + \text{Re}(T)]$
		T_3^+	$\text{Im}(\chi_{YY,ZZ}) = -\frac{1}{16}[2 \text{Im}(P) + \text{Im}(J) - \text{Im}(M) + \text{Im}(Q) - \text{Im}(T)]$
	YZ	None	$\text{Re}(\chi_{YZ,ZY}) = \frac{1}{32}[C - E + F - G - 2\text{Re}(U) + 2\text{Re}(V)]$
		T_3^+	$\text{Im}(\chi_{YZ,ZY}) = 0$

$U(II, YY)$	II	None	$\text{Re}(\chi_{II,YY}) = \frac{1}{16}[B - D + \text{Re}(J) - \text{Re}(M) - \text{Re}(Q) + \text{Re}(T)]$
		T_4^+	$\text{Im}(\chi_{II,YY}) = \frac{1}{16}[2 \text{Im}(P) - \text{Im}(J) + \text{Im}(M) - \text{Im}(Q) + \text{Im}(T)]$
	IX	T_4^+	$\text{Re}(\chi_{IX,YZ}) = \frac{1}{16}[\text{Re}(U) + \text{Re}(V)]$
		None	$\text{Im}(\chi_{IX,YZ}) = -\frac{1}{32}(C - E - F + G)$
	IY	None	$\text{Re}(\chi_{IY,YI}) = \frac{1}{32}[C - E + F - G + 2\text{Re}(U) + 2\text{Re}(V)]$
		T_4^+	$\text{Im}(\chi_{IY,YI}) = 0$
	XI	T_4^+	$\text{Re}(\chi_{XI,ZY}) = \frac{1}{16}[\text{Im}(X) + \text{Im}(Y)]$
		None	$\text{Im}(\chi_{XI,ZY}) = -\frac{1}{32}(C - E - F + G)$
	XX	None	$\text{Re}(\chi_{XX,ZZ}) = -\frac{1}{16}[-B + D + \text{Re}(J) - \text{Re}(M) - \text{Re}(Q) + \text{Re}(T)]$
		T_4^+	$\text{Im}(\chi_{XX,ZZ}) = -\frac{1}{16}[2 \text{Im}(P) + \text{Im}(J) - \text{Im}(M) + \text{Im}(Q) - \text{Im}(T)]$
	XZ	None	$\text{Re}(\chi_{XZ,ZX}) = \frac{1}{32}[C - E + F - G - 2\text{Re}(U) + 2\text{Re}(V)]$
		T_4^+	$\text{Im}(\chi_{XZ,ZX}) = 0$

$U(II, ZZ)$	II	None	$\text{Re}(\chi_{II,ZZ}) = \frac{1}{16}[1 + A - B - D + 2\text{Re}(L) - 2\text{Re}(P)]$
		T_5^+	$\text{Im}(\chi_{II,ZZ}) = \frac{1}{16}[2 \text{Im}(J) + 2\text{Im}(M) - 2\text{Im}(Q) - 2\text{Im}(T)]$
	IX	T_5^+	$\text{Re}(\chi_{IX,ZY}) = -\frac{1}{16}[\text{Im}(U) - \text{Im}(V)]$
		None	$\text{Im}(\chi_{IX,ZY}) = \frac{1}{32}(C + E - F - G)$
	IY	T_5^+	$\text{Re}(\chi_{IY,ZX}) = \frac{1}{16}[\text{Im}(U) - \text{Im}(V)]$
		None	$\text{Im}(\chi_{IY,ZX}) = -\frac{1}{32}(C + E - F - G)$
	IZ	None	$\text{Re}(\chi_{IZ,ZI}) = \frac{1}{16}[1 + A - 2\text{Re}(L)]$
		T_5^+	$\text{Im}(\chi_{IZ,ZI}) = 0$
	XI	T_5^+	$\text{Re}(\chi_{XI,YZ}) = -\frac{1}{16}[\text{Im}(U) - \text{Im}(V)]$
		None	$\text{Im}(\chi_{XI,YZ}) = \frac{1}{32}(C + E - F - G)$
	YI	T_5^+	$\text{Re}(\chi_{YI,XZ}) = -\frac{1}{16}[\text{Im}(U) + \text{Im}(V)]$
		None	$\text{Im}(\chi_{YI,XZ}) = -\frac{1}{32}(C + E - F - G)$
	XX	None	$\text{Re}(\chi_{XX,YY}) = \frac{1}{16}[B + D - H - 2\text{Re}(P)]$
		T_5^+	$\text{Im}(\chi_{XX,YY}) = 0$
	XY	None	$\text{Re}(\chi_{XY,YX}) = \frac{1}{16}H$
		T_5^+	$\text{Im}(\chi_{XY,YX}) = 0$

$U(IX, YI)$	II	None	$\text{Re}(\chi_{IX, YI}) = 0$
		T_6^+	$\text{Im}(\chi_{IX, YI}) = \frac{1}{32}[C - E + F - G + 2\text{Im}(U) + 2\text{Im}(V)]$
	XI	T_6^+	$\text{Re}(\chi_{XX, ZI}) = -\frac{1}{16}[\text{Re}(J) - \text{Re}(M) + \text{Re}(Q) - \text{Re}(T)]$
		None	$\text{Im}(\chi_{XX, ZI}) = -\frac{1}{16}[\text{Im}(J) - \text{Im}(M) + \text{Im}(Q) - \text{Im}(T)]$
	XX	T_6^+	$\text{Re}(\chi_{XI, ZX}) = -\frac{1}{32}(C - E - F + G)$
		None	$\text{Im}(\chi_{XI, ZX}) = -\frac{1}{16}[\text{Im}(U) + \text{Im}(V)]$
	XY	T_6^+	$\text{Re}(\chi_{XZ, ZY}) = 0$
		None	$\text{Im}(\chi_{XZ, ZY}) = -\frac{1}{32}[C + E + F + G - 2\text{Im}(U) + 2\text{Im}(V)]$
	YY	T_6^+	$\text{Re}(\chi_{IY, YZ}) = -\frac{1}{32}(C - E - F + G)$
		None	$\text{Im}(\chi_{IY, YZ}) = -\frac{1}{16}[\text{Im}(U) + \text{Im}(V)]$
	YZ	T_6^+	$\text{Re}(\chi_{YI, IZ}) = -\frac{1}{16}[\text{Re}(J) - \text{Re}(M) + \text{Re}(Q) - \text{Re}(T)]$
		None	$\text{Im}(\chi_{YI, IZ}) = -\frac{1}{16}[-\text{Im}(J) + \text{Im}(M) + \text{Im}(Q) - \text{Im}(T)]$

$U(IY, XI)$	II	None	$\text{Re}(\chi_{IY, XI}) = 0$
		T_7^+	$\text{Im}(\chi_{IY, XI}) = -\frac{1}{32}[C - E + F - G + 2\text{Re}(U) + 2\text{Re}(V)]$
	IX	T_7^+	$\text{Re}(\chi_{IZ, XX}) = -\frac{1}{16}[\text{Re}(J) - \text{Re}(M) + \text{Re}(Q) - \text{Re}(T)]$
		None	$\text{Im}(\chi_{IZ, XX}) = -\frac{1}{16}[-\text{Im}(J) + \text{Im}(M) + \text{Im}(Q) - \text{Im}(T)]$
	IZ	T_7^+	$\text{Re}(\chi_{IX, XZ}) = \frac{1}{32}(C - E - F + G)$
		None	$\text{Im}(\chi_{IX, XZ}) = \frac{1}{16}[\text{Im}(U) + \text{Im}(V)]$
	YI	T_7^+	$\text{Re}(\chi_{YI, ZI}) = \frac{1}{16}[\text{Re}(J) - \text{Re}(M) + \text{Re}(Q) - \text{Re}(T)]$
		None	$\text{Im}(\chi_{YI, ZI}) = \frac{1}{16}[\text{Im}(J) - \text{Im}(M) + \text{Im}(Q) - \text{Im}(T)]$
	YX	None	$\text{Re}(\chi_{YZ, ZX}) = 0$
		T_7^+	$\text{Im}(\chi_{YZ, ZX}) = \frac{1}{32}[C - E + F - G - 2\text{Re}(U) - 2\text{Re}(V)]$
	YY	T_7^+	$\text{Re}(\chi_{YI, ZY}) = \frac{1}{32}(C - E - F + G)$
		None	$\text{Im}(\chi_{YI, ZY}) = \frac{1}{16}[\text{Im}(U) + \text{Im}(V)]$

$U(IY, ZY)$	II	None	$\text{Re}(\chi_{IY, ZY}) = \frac{1}{32}(C + E - F - G)$
		T_8^+	$\text{Im}(\chi_{IY, ZY}) = \frac{1}{16}[\text{Im}(U) - \text{Im}(V)]$
	IX	None	$\text{Re}(\chi_{IZ, ZZ}) = -\frac{1}{16}[A - 1 - \text{Re}(J) - \text{Re}(M) + \text{Re}(Q) + \text{Re}(T)]$
		T_8^+	$\text{Im}(\chi_{IZ, ZZ}) = -\frac{1}{16}[-2\text{Im}(L) + \text{Im}(J) + \text{Im}(M) + \text{Im}(Q) + \text{Im}(T)]$
	XX	T_8^+	$\text{Re}(\chi_{XZ, YZ}) = 0$
		None	$\text{Im}(\chi_{XZ, YZ}) = -\frac{1}{32}[C + E + F + G - 2\text{Re}(U) + 2\text{Re}(V)]$
